Chemical Science

ROYAL SOCIETY OF CHEMISTRY

EDGE ARTICLE

View Article Online
View Journal | View Issue

Check for updates

Cite this: *Chem. Sci.*, 2022, **13**, 4131

All publication charges for this article have been paid for by the Royal Society of Chemistry

Received 17th January 2022
Accepted 15th March 2022

DOI: 10.1039/d2sc00313a

rsc.li/chemical-science

Diaryliodonium salts facilitate metal-free mechanoredox free radical polymerizations†

Sarah M. Zeitler, ‡ Progyateg Chakma ‡ and Matthew R. Golder *

Mechanically-induced redox processes offer a promising alternative to more conventional thermal and photochemical synthetic methods. For macromolecule synthesis, current methods utilize sensitive transition metal additives and suffer from background reactivity. Alternative methodology will offer exquisite control over these stimuli-induced mechanoredox reactions to couple force with redox-driven chemical transformations. Herein, we present the iodonium-initiated free-radical polymerization of (meth)acrylate monomers under ultrasonic irradiation and ball-milling conditions. We explore the kinetic and structural consequences of these complementary mechanical inputs to access high molecular weight polymers. This methodology will undoubtedly find broad utility across stimuli-controlled polymerization reactions and adaptive material design.

Introduction

Mechanochemistry[1–5] is an interdisciplinary field spanning small molecule methodology, crystal engineering, and polymer science. Chemical processes induced by mechanical force offer advantages over other stimuli. For example, undesirable thermal byproducts can be avoided and limited stimuli penetration (*e.g.*, photochemistry) into solutions can be mitigated.[1,5] For macromolecules, force-responsive polymers with engineered mechanophores[6,7] can change color,[8] alter bulk electronic[9] or structural[10–13] properties, and release cargo[14,15] on demand *via* mechanochemically-driven processes; such systems find utility in sensing,[10] additive manufacturing,[16,17] and therapeutic delivery[18,19] applications. One common form of mechanochemical input is ultrasound (US) irradiation.[20] Ultrasonic waves generate cavitation bubbles[21] that collapse and produce forces that fuel subsequent processes. US itself is readily accessible and has numerous biological applications[22–24] in diagnostic imaging[25] and targeted drug release.[26,27] A complimentary method to generate force in mechanochemical systems is ball milling, a sustainable and economical technique due to the removal of nearly all solvent.[3] This industrially scalable technology was originally developed for the breakdown of minerals and biopolymers[28] but recently became a widespread method for solid-state synthesis.[3,29] The ubiquity of force-induced macromolecular deconstruction largely dominates the field of mechanochemistry. Counterintuitively, analogous systems also exist that construct matter[30] *via* covalent bond formations under mechanical stimulation.

One mechanism to facilitate the use of force in chemical synthesis is mechanoredox catalysis[31] (Fig. 1); the piezoelectric

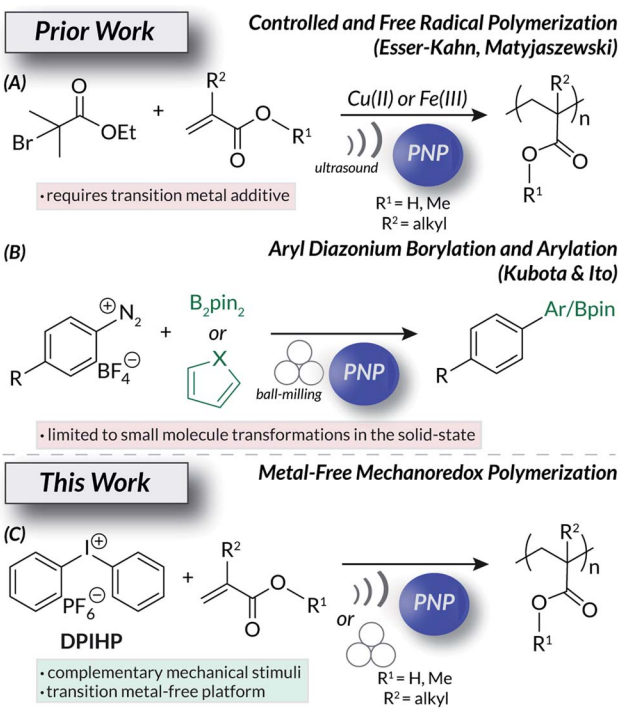

Fig. 1 Evolution of (A) mechanoredox polymerizations and (B) small molecule transformations (*e.g.*, borylation, arylation) as an inspiration for (C) our metal-free ultrasonic irradiation and ball-milling mechanoredox polymerization methodology.

Department of Chemistry, Molecular Engineering & Science Institute, University of Washington, 36 Bagley Hall, Seattle, WA 98195, USA. E-mail: goldermr@uw.edu

† Electronic supplementary information (ESI) available: Experimental details, additional control experiments, photographs of experimental setups, NMR spectra. See DOI: 10.1039/d2sc00313a

‡ Equal contribution.

Open Access Article. Published on 16 March 2022. Downloaded on 2/9/2026 10:15:19 PM.
This article is licensed under a Creative Commons Attribution-NonCommercial 3.0 Unported Licence.

Open Access Article. Published on 16 March 2022. Downloaded on 2/9/2026 10:15:19 PM.
This article is licensed under a Creative Commons Attribution-NonCommercial 3.0 Unported Licence.

effect[32–35] converts mechanical energy into a useable electric potential. Many applications mirror bone growth[36] and mechanogenetics[24,37] mechanisms found in biological systems. Other uses of piezoelectric materials and molecules include water splitting and treatment;[38–41] wearable devices have even been developed to use piezoelectricity as a means to couple human motion with energy storage.[42] Only recently have chemists utilized this concept in modern synthetic polymer chemistry (*i.e.*, mechanoredox catalysis). Several examples now exist that harness US and the piezoelectric effect to drive mechanoredox polymerization processes (Fig. 1A).[31] Both the Esser-Kahn and Matyjaszewski groups have developed systems where piezoelectric nanoparticles (PNP) facilitate either free radical polymerization (FRP) or atom transfer radical polymerization (ATRP) in the presence of US.[43–46] While both works demonstrate the feasibility of mechanoredox polymerizations, these methods require transition metal additives (*e.g.*, copper or iron salts)[44,45] and have significant non-mechanoredox background reactions.[43,44] The current state of the art leaves vast opportunities to further refine mechanoredox polymerization methodology. Such fundamental developments are imperative to the development and implementation of next-generation stimuli-responsive soft materials.

PNPs can also be used to drive small molecule mechanoredox transformations. In recent work by Kubota and Ito, ball-milling with PNPs (*e.g.*, ZnO, $BaTiO_3$) initiates C–H borylations and arylation reactions (Fig. 1B).[47] Similar solid-state techniques also effect aryl trifluoromethylation[48] and atom-transfer radical cyclization reactions.[49] Interestingly, mechanoredox radical polymerizations have never been initiated under ball-milling conditions. In the initial small molecule mechanoredox study by Kubota and Ito, aryl diazonium salts were used as "initiators" to drive the subsequent radical C–H functionalization reactions.[47] These salts, along with other aryl onium salts (*e.g.*, diaryl iodoniums and triaryl sulfoniums) have been used in photoredox systems as tunable aryl radical[50] surrogates with varying reduction potentials;[51] aryl diazoniums are extremely labile while diaryl iodoiniums and triaryl sulfoniums ($E_{red} = -0.3$ V to -1.0 V *vs.* SCE) are significantly less susceptible to reduction. The reactivity of onium salts can be further manipulated through substituent effects, leading to a wide array of reactivity.[52] Many onium salts are also either commercially available or readily synthesized, making them accessible, bench-stable building blocks for synthetic manipulations. Furthermore, onium salts can be used to integrate soft materials with surfaces, presenting opportunities for tuneable polymer grafting and composites.[53,54]

Using these recent works as inspiration, we now report the mechanoredox onium salt-initiated FRP of (meth)acrylates under both ultrasonic irradiation and ball-milling conditions (Fig. 1C). This work details the first examples of metal-free mechanoredox polymerizations and compares the consequences of these conditions under complementary reaction conditions (*i.e.*, ultrasonic irradiation and ball-milling). Overall, we demonstrate the broad application of mechanical force to access industrially relevant high molecular weight polymeric materials without relying on traditional thermal[55–57] or photochemical[58–61] inputs.

Results & discussion

Ultrasonic irradiation (US) mechanoredox polymerizations

Inspired by the work[47] of Kubota and Ito, we initially wondered whether aryl diazonium salts could be used as mechanoredox initiators for FRP of commercially available acrylates. To investigate, 4-bromobenzenediazonium tetrafluoroborate (BBDT) and 4-methoxybenzenediazoium tetrafluoroborate (MBDT) were used as initiators in the presence of a suitable PNP (*e.g.*, ZnO or $BaTiO_3$) and acrylate monomer. Degassed reaction mixtures were immersed into a thermostated ultrasonic bath (see Fig. S1† for a typical reaction setup); to our surprise, while high monomer conversion was achieved in a variety of different organic solvents in the presence of both US and PNPs, similar results were obtained in the absence of US (Table S1†). Despite numerous examples employing BBDT or MBDT as aryl radical precursors in photoredox processes,[51] we found after extensive studies that aryl diazoniums were too capricious to use in this system. The background reactions in the absence of force affirm that even a low concentration of radicals, presumably from aryl diazonium decomposition in solution, can initiate FRP. These early studies prompted us to investigate alternative onium salts with more negative reduction potentials; we rationalized that such initiators would exhibit superior solution-state stability.

We hypothesized that diaryliodonium salts,[62] which are more difficult to reduce (E_{red} = *ca.* -0.5 V *vs.* SCE) and thus should be more stable in solution than aryl diazonium salts, would be more suitable for mechanoredox FRP. To explore this new system, we first studied the polymerization of *tert*-butyl acrylate (*t*BA) in DMF by using diphenyl iodonium hexafluorophosphate (DPIHP) as our initiator (Table 1) with either

Table 1 Importance of nanoparticle identity for mechanoredox *t*BA FRP[a]

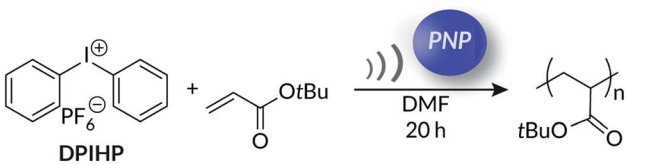

Entry[b]	Nanoparticle	Ultrasound?	Conversion[c] (%)
1	$BaTiO_3$ (1.5 wt%)	Yes	35
2	$BaTiO_3$ (3.5 wt%)	Yes	80
3	$BaTiO_3$ (7 wt%)	Yes	92
4	$BaTiO_3$ (7 wt%)	No	<5
5	ZnO (7 wt%)	Yes	70
6	TiO_2 (7 wt%)	Yes	17
7	None	Yes	14

[a] Reaction conditions: $[monomer]_0 : [DPIHP]_0 = 100 : 1$. [b] [*t*BA] = 7.3 M, [DPIHP] = 0.073 M in DMF. [c] Conversion was determined by ^{1}H NMR spectroscopy. Ultrasonic bath (40 kHz, 70 W, 20 °C); reaction time: 20 h.

© 2022 The Author(s). Published by the Royal Society of Chemistry

Open Access Article. Published on 16 March 2022. Downloaded on 2/9/2026 10:15:19 PM. This article is licensed under a Creative Commons Attribution-NonCommercial 3.0 Unported Licence.

$BaTiO_3$ or ZnO (Table 1, entries 1–5) as the PNP. With both PNPs, the reaction mixtures became visibly viscous within 8 h of sonication, suggesting high monomer conversion (see Fig. S2† representative photographs). In the presence of 7 wt% $BaTiO_3$ and ZnO (relative to the combined mass of the monomer, solvent, and DPIHP), ^{1}H NMR analysis of the resulting polymers showed 92% and 68% monomer conversion after 20 h, respectively. In the absence of US or PNP, however, little to no conversion was seen over the same time period. A direct correlation of PNP loading to monomer conversion was observed, indicating the pivotal role of nanoparticles. Maximum monomer conversion was achieved with 7 wt% PNP, so this loading was used for all future experiments. Results remained consistent with high monomer conversion on larger scale (10x scale = 5 g *t*BA monomer) using $BaTiO_3$ (Fig. S5†), highlighting the potential scalability of ultrasonic irradiation mechanoredox polymerizations.

Intriguingly, in the absence of either US (Table 1, entry 4) or PNP (Table 1, entry 7), no visual change to the reaction mixture was observed and little to no conversion was measured by ^{1}H NMR spectroscopy. Similar results (Fig. S2†) were obtained when a neutral non-PNP (TiO_2) was used (Table 1, entry 6). Based on these results, we surmised that solvent played a key role in the background processes (Table 1, entries 6 & 7) observed. While the exact nature of all initiating species is not fully clear, these collective data demonstrate the importance of iodonium salt for efficient polymerization.

We postulated that the trivial conversion (*ca.* 15%) measured in the absence of PNPs could be attributed to solvent initiated polymerization (Fig. S3 and S4†). Organic solvent radicals are known to form in response to high frequency US (*ca.* 500 kHz); subsequent homolytic C–C, C–N, or C–H bond cleavage forms species that can initiate radical polymerization.[63–67] Unfortunately, the role of solvent radicals in background reactions are often overlooked in recent mechanoredox polymerization reports. To examine whether low frequency (40 kHz) US-mediated solvent radical generation can also induce significant polymerization, control experiments were conducted where *t*BA was sonicated in different organic solvents without PNP and DPIHP. A maximum monomer conversion of 15% was observed over 20 h (Table S2†), suggesting that although certain solvents can generate radicals in response to low frequency US (40 kHz), the local concentration of active initiator is not sufficient to achieve high monomer conversion.

While the importance of PNPs is already established (Table 2, entry 1), additional control experiments were necessary to further probe the polymerization mechanism. When the DPIHP initiator was removed from the reaction mixture, less than 15% monomer conversion was observed in 20 h (Table 2, entry 2). The trivial monomer conversion can be attributed to US-mediated solvent radical polymerization (*vide supra*) and confirms the significant role the diaryliodonium salt plays in the observed US-mechanoredox FRPs. This result was corroborated with a simple kinetics experiment; *t*BA and $BaTiO_3$ were sonicated in DMF without DPIHP for 8 h and ~10% conversion was observed by ^{1}H NMR spectroscopy. Upon addition of DPIHP to this reaction mixture, >90% monomer conversion was observed after an additional 12 h (20 h total reaction time) (Fig. S6†). Additionally, when polymerizations were run without exclusion of air (Table 2, entry 3) or with 1 equiv. of radical inhibitor 4-methoxyphenol (MEHQ) (Table 2, entry 4), <5% conversion was observed, supporting the envisaged free-radical mechanism.

To further optimize reaction conditions, we then evaluated solvent scope in the mechanoredox polymerization of *t*BA (Table S3†). In general, >30% monomer conversion was observed in polar aprotic organic solvents (*i.e.*, DMF, DMAc, DMSO, 1,4-dioxane) but no conversion was observed in non-polar solvents (*i.e.*, toluene, anisole). These differences are likely in part due to poor DPIHP solubility in less polar solvents. In all cases, <5% conversion was observed in the absence of US (Table S4†). Additionally, when US-mechanoredox FRP was carried out in anhydrous solvent, no significant difference in monomer conversion was observed, confirming minimal radical generation from water.[67–69] Overall, higher monomer conversion was achieved using $BaTiO_3$ than with ZnO. Based upon these cumulative results (Table S3†), $BaTiO_3$/DMF and ZnO/DMAc were used for the remainder of the studies reported below.

Table 2 US-mechanoredox *t*BA polymerization control experiments[a]

Entry	Conditions	Conversion[c] (%)
1[b]	Standard reaction	92
2	Without DPIHP	14
3	Under air	<5
4	MEHQ (1 : 1 eq. to DPIHP)	<5

[a] Reaction conditions: $[monomer]_0 : [DPIHP]_0 = 100 : 1$. [b] [*t*BA] = 7.3 M, [DPIHP] = 0.073 M in DMF, 7 wt% $BaTiO_3$. [c] Conversion was determined by ^{1}H NMR spectroscopy. Ultrasonic bath (40 kHz, 70 W, 20 °C); reaction time: 20 h.

Table 3 Results for US-mechanoredox (meth)acrylate FRP[a]

Entry	Monomer	Nanoparticle	Conversion[e] (%)	M_n[f] (kDa)	$Đ$[f]
1[b]	*t*BA	$BaTiO_3$	92	284	1.7
2[b]	*t*BA	ZnO	68	347	1.6
3[b]	BA	$BaTiO_3$	82	431	1.8
4[b]	BA	ZnO	56	358	1.7
5[c]	EA	$BaTiO_3$	64	491	1.5
6[c]	EA	ZnO	51	533	1.5
7[d]	MA	$BaTiO_3$	78	1230	1.8
8[d]	MA	ZnO	32	357	2.0
9[c]	MMA	$BaTiO_3$	38	105	1.7
10[c]	MMA	ZnO	35	107	1.5

[a] Reaction conditions: $[monomer]_0 : [DPIHP]_0 = 100 : 1$. [b] [monomer] = 7.3 M, [DPIHP] = 0.073 M. [c] [monomer] = 9.3 M, [DPIHP] = 0.093 M. [d] [monomer] = 10.9 M, [DPIHP] = 0.109 M. DMF and DMAc were used as solvents for mechanoredox reactions with $BaTiO_3$ and ZnO, respectively. [e] Conversion was determined by ^{1}H NMR spectroscopy. [f] M_n and $Đ$ were determined by GPC-MALS. 7 wt% nanoparticle loading was used for all reactions. Ultrasonic bath (40 kHz, 70 W). Reaction time: 20 h.

Open Access Article. Published on 16 March 2022. Downloaded on 2/9/2026 10:15:19 PM.
This article is licensed under a Creative Commons Attribution-NonCommercial 3.0 Unported Licence.

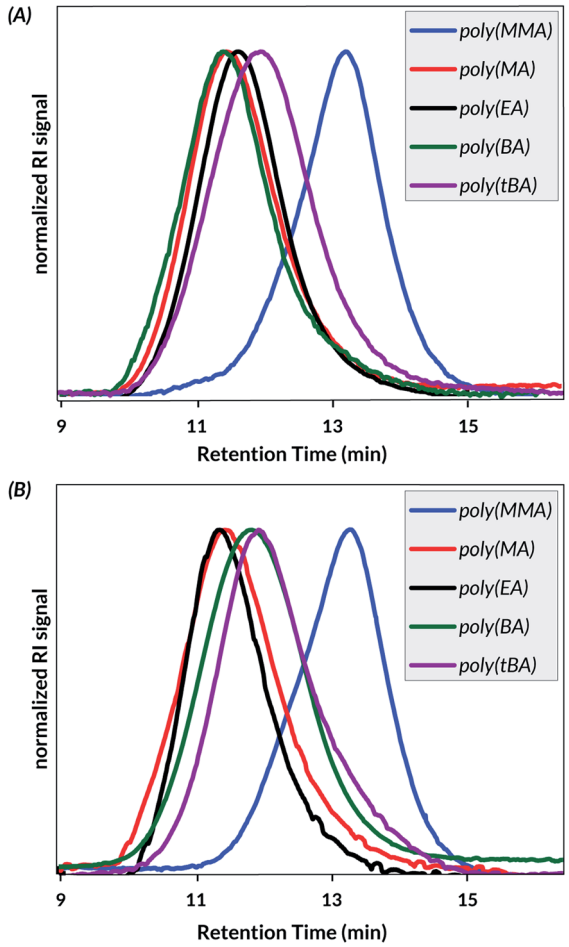

Fig. 2 GPC-RI traces of US-mechanoredox (meth)acrylate FRP using (A) $BaTiO_3$ or (B) ZnO as the PNP (see Table 3).

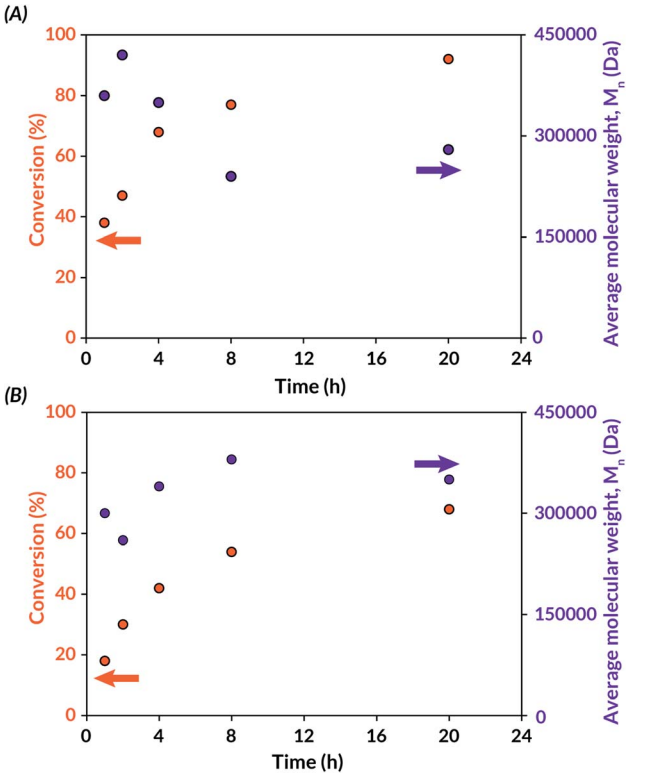

Fig. 3 Conversion and molar mass progression during US-mechanoredox *t*BA polymerizations under optimized conditions (see Table 3): (A) with $BaTiO_3$ (7 wt%) in DMF; (B) with ZnO (7 wt%) in DMAc.

Next, to study the viability of the optimized conditions with other monomers, the mechanoredox polymerizations of butyl acrylate (BA), ethyl acrylate (EA), methyl acrylate (MA), and methyl methacrylate (MMA) were studied. The resulting monomer conversions (Table 3 and Fig. 3A) reveal consistently higher conversions of $BaTiO_3$ reactions over ZnO reactions (Table 3 and Fig. 3B) and acrylates over methacrylates. The number average molecular weights (M_n), and dispersity ($Đ = M_w/M_n$) data measured by gel permeation chromatography coupled with a multi-angle light scattering detector (GPC-MALS) reveals high molecular weight (>100 kDa) polymer with little control over dispersity as is expected from a conventional mechanoredox FRP process (Fig. 2). Again, no polymerization was observed when reactions were carried out in the absence of US (Table S5†).

Finally, *t*BA mechanoredox polymerization kinetics were studied, and the resulting data were analysed by ^{1}H NMR spectroscopy and GPC-MALS. Within the 20 h reaction window, a time dependent progression of polymer formation was observed. Polymerizations were faster with $BaTiO_3$ than with ZnO at all analysed time points. In both cases, high molecular weight polymer was observed from GPC-MALS traces, indicating fast propagation rates relative to initiation rates. To study whether any decrease in M_n over time (Fig. 3) was due to mechanochemical polymer cleavage,[70] US-mediated chain scission experiments were carried out on DMF solutions of freshly synthesized poly(*t*BA) and poly(MMA). After sonication for 24 h, analysis of the resulting materials by GPC-MALS (Fig. S7†) indicated that mechanochemical chain scission is operative at extended reaction times. For example, 170 kDa poly(*t*BA) synthesized through US-mechanoredox FRP was reduced to 21 kDa after prolonged ultrasonication. Hence, we believe that the observed molecular weight evolutions (Fig. 3) likely are complicated through competing propagation and chain scission pathways.

Additionally, an "on–off" experiment was conducted to assess the role of US on the FRP reaction profile (Fig. S8†). As assessed by ^{1}H NMR spectroscopy, *t*BA conversion reached 35% after 1 h of US and remained stagnant (<5% further conversion) during the first "off" period of 2 h. During the second 2 h "on" period, monomer conversion increased to 57%. Interestingly, after a longer "off" period (15 h), monomer conversion increased to 73%. These data collectively suggest that while FRP rates are higher in the presence of US, likely due to continuous mechanoredox generation of initiating radicals and/or thermal cavitation effects under US irradiation, propagating chain ends still remain active even in the absence of US.

Ball-milling (BM) mechanoredox polymerizations

As the diaryl iodonium chemistry evolved in solution using ultrasound, we were intrigued to find out if mechanoredox FRP

© 2022 The Author(s). Published by the Royal Society of Chemistry

Open Access Article. Published on 16 March 2022. Downloaded on 2/9/2026 10:15:19 PM.
This article is licensed under a Creative Commons Attribution-NonCommercial 3.0 Unported Licence.

could transition into the ball mill. The advantages of ball-milling, including reducing solvent usage, mitigating reagent insolubility,[71] and facilitating the use of incompatible and/or immiscible reagents,[72] are apparent from prior BM step-growth,[73] ring-opening,[74] and iterative[75] polymerizations. Although poly(meth)acrylates have been accessed under ball-milling conditions *via* mechanochemical radical generation on quartz surfaces[76] and a recapitulated solid-state ATRP process,[77] the use of a tuneable mechanoredox pathway has remained unrealized under ball milling conditions prior to our work.

To begin, we translated our optimized US-mechanoredox FRP conditions for *t*BA (50 : 1 *t*BA : DPIHP, 7 wt% $BaTiO_3$) into the ball mill using minimal DMF (0.12 mL, 0.030% v/w = volume of DMF relative to total mass of all other reaction components) as is required for liquid assisted grinding (LAG).[78] LAG is a procedure that enhances mechanochemical reactivity through the addition of small quantities of a solvent.[3] Upon initial investigation, >95% monomer conversion was observed by ^{1}H NMR spectroscopy (Fig. S9†) after only 3 h in the ball mill (30 Hz) compared to 20 h in solution with US; the resulting material in the stainless steel milling jar was a visibly viscous material (Fig. S10†) with a high molecular weight (M_n = 165 kDa) as determined by GPC-MALS. Unlike the US-mediated reactions, ball-milling was tolerant of oxygen and rigorous exclusion of air was not required. Our observations are in stark contrast to Bielawski's recent work on solid-state ATRP[77] where polymerization only occurred in an inert atmosphere. Other common acrylates also showed high conversions (Table 4) under our BM-mechanoredox FRP conditions, but importantly, monomer conversion was seen only when samples were subjected to ball-milling. As with the US processes, both onium salt and PNP were required; when DPIHP and/or $BaTiO_3$ were removed from the reaction mixture, no monomer conversion was observed (Table S6†). Similarly, when the PNP was replaced with TiO_2, no conversion was seen after ball-milling for 3 h (Table S7†).

Table 4 Ball-milling mechanoredox acrylate polymerizations[a]

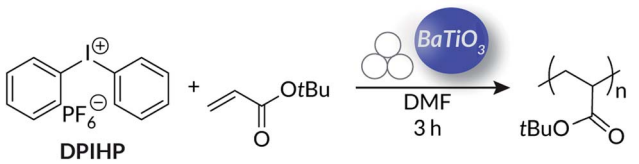

Entry	Monomer	Conversion[b] (%)	M_n [c] (kDa)	$Đ$[c]
1	*t*BA	>95	416	1.3
2	BA	90	556	1.6
3	EA	>95	751	1.4
4	MA	>95	937	1.2
5	MMA	86	56.0	1.7

[a] Reaction conditions: monomer = 2.0 mmol, DPIHP = 0.040 mmol, $BaTiO_3$ = 0.60 mmol, DMF (for LAG) = 0.12 mL (0.030% v/w). [b] Conversion was determined by ^{1}H NMR spectroscopy. [c] M_n and $Đ$ were determined by GPC-MALS. Ball mill (1.5 mL stainless steel jar, 5 mm stainless steel grinding ball, 30 Hz). Reaction time: 3 h.

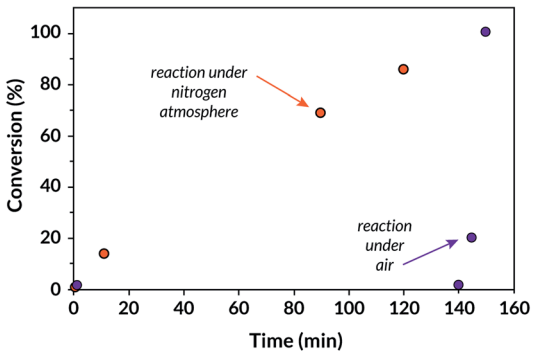

Fig. 4 Comparison of BM-mechanoredox kinetics (*t*BA conversion) in an inert atmosphere and under air.

We then investigated the kinetics of BM-mechanoredox FRP due to their expedited rates compared to our US-mediated FRP. Interestingly, these studies revealed that there is an incubation period; no conversion is observed prior to 140 minutes (Fig. 4). Since these reactions are conducted under air in sealed vessels, we hypothesized that the limited oxygen would eventually be removed from the atmosphere, potentially through reduction under mechanoredox conditions. Once the atmosphere is "scrubbed" of oxygen, nearly quantitative monomer conversion is quickly observed after just an additional *ca.* 10 min. To test this hypothesis, we set up a *t*BA BM-mechanoredox FRP reaction under an inert N_2 atmosphere in a glovebox and observed that FRP proceeded without a noticeable incubation period (Table S8†). 14% conversion was observed after just 10 minutes while nearly 70% conversion was observed after 90 minutes. Oxygen seems to perturb the onset of monomer conversion but does not significantly affect the overall time to full conversion (*ca.* 150 min). We surmise that mixing is the rate limiting factor under inert conditions; in the presence of oxygen, sufficient mixing becomes competitive with atmosphere scrubbing so monomer consumption appears to be nearly instantaneous once all oxygen is removed from the system.

The overall physical data collected from GPC-MALS analysis (Table 4 and Fig. S11†) of BM-mechanoredox FRP polymers show similar trends to what was measured for US-mechanoredox FRP. Importantly, the similarities in M_n and $Đ$ between the two methods suggest that ball-milling leads to uniform rate enhancements (*i.e.* rates of initiation, propagation, and termination) relative to US; drastic disparities in M_n and/or $Đ$ would suggest non-uniform rate enhancements in the ball mill. Under an inert atmosphere, >90% monomer consumption is achieved in under 3 h *via* ball-milling conditions, while almost a full day (20 h) reaction is needed under ultrasonic irradiation conditions. Hence, solvating conditions (*i.e.* US-mechanoredox FRP) slow the overall rate of monomer consumption compared to that of BM-mechanoredox FRP, but do not significantly alter the makeup of the final poly(meth) acrylates. Interestingly, resubjection of BM-mechanoredox

Open Access Article. Published on 16 March 2022. Downloaded on 2/9/2026 10:15:19 PM. This article is licensed under a Creative Commons Attribution-NonCommercial 3.0 Unported Licence.

polymers (*e.g.*, poly(*t*BA), poly(MMA)) to the original reaction conditions (0.030% v/w DMF, ball-milling at 30 Hz, 3 h) led to only a small decrease in molar mass as assessed by GPC-MALS (Fig. S12 and S13†). Hence, while mechanochemical chain scission pathways were operative under ultrasonication conditions, they were less prevalent, at least on this shorter time scale, under ball-milling conditions.

Based on work from the ultrasonic irradiation reactions, we hypothesized that PNP identity may also influence polymerization efficiency. Upon testing this hypothesis, we determined that the difference in reactivity between the two PNPs in ball-milling is much more significant than with US. Under otherwise identical conditions (Table 4), no conversion was observed when $BaTiO_3$ was replaced with ZnO (Table S7†). These results parallel the trends observed in C–H borylation and arylation reactions studied by Kubota and Ito;[47] the specific mechanistic underpinnings behind such a stark reactivity difference is unclear at this time.

Conclusions

In summary, we developed mechanoredox methodology for the synthesis of poly(meth)acrylates under complementary reaction conditions. The fields of self-healing and strain-strengthening materials will undoubtedly benefit from fundamental processes that can forge chemical bonds in response to mechanical inputs. In fact, several examples of mechanoredox polymer crosslinking[79–81] already exist, providing compelling arguments for accessing thermoset materials that may be inaccessible under thermal conditions. Furthermore, as photons are readily absorbed by chromophores or scattered by insoluble additives,[82,83] the ability to spatially focus mechanical energy will allow for the development of advanced, responsive macromolecular networks. The diversity of mechanical inputs provides the opportunity for divergent applications as the field evolves. Additional mechanistic studies are ongoing in our lab to probe experimental differences observed in these mechanoredox FRP studies and the exact identity of initiating species.

Author contributions

S. M. Z. and P. C. contributed equally. S. M. Z. and P. C. conducted ultrasonic irradiation mechanoredox polymerizations; S. M. Z. conducted ball-milling mechanoredox polymerizations. All authors analysed and discussed experimental data. S. M. Z., P. C., and M. R. G. wrote the manuscript; all authors discussed and edited the manuscript.

Conflicts of interest

There are no conflicts to declare.

Acknowledgements

The authors thank the University of Washington for generous startup funds. This work was supported in part by a seed grant from UW MEM-C, an NSF MRSEC funded under DMR-1719797.

Notes and references

1 J. L. Howard, Q. Cao and D. L. Browne, *Chem. Sci.*, 2018, **9**, 3080–3094.
2 J. A. Leitch and D. L. Browne, *Chem.–Eur. J.*, 2021, **27**, 9721–9726.
3 T. Friščić, C. Mottillo and H. M. Titi, *Angew. Chem., Int. Ed.*, 2019, 2–14.
4 R. T. O'Neill and R. Boulatov, *Nat. Rev. Chem.*, 2021, **5**, 148–167.
5 J. L. Do and T. Friščić, *ACS Cent. Sci.*, 2017, **3**, 13–19.
6 M. M. Caruso, D. A. Davis, Q. Shen, S. A. Odom, N. R. Sottos, S. R. White and J. S. Moore, *Chem. Rev.*, 2009, **109**, 5755–5798.
7 D. A. Davis, A. Hamilton, J. Yang, L. D. Cremar, D. Van Gough, S. L. Potisek, M. T. Ong, P. V. Braun, T. J. Martínez, S. R. White, J. S. Moore and N. R. Sottos, *Nature*, 2009, **459**, 68–72.
8 M. E. McFadden and M. J. Robb, *J. Am. Chem. Soc.*, 2019, **141**, 11388–11392.
9 Z. Chen, J. A. M. Mercer, X. Zhu, J. A. H. Romaniuk, R. Pfattner, L. Cegelski, T. J. Martinez, N. Z. Burns and Y. Xia, *Science*, 2017, **357**, 475–479.
10 C. L. Brown and S. L. Craig, *Chem. Sci.*, 2015, **6**, 2158–2165.
11 C. E. Diesendruck, G. I. Peterson, H. J. Kulik, J. A. Kaitz, B. D. Mar, P. A. May, S. R. White, T. J. Martínez, A. J. Boydston and J. S. Moore, *Nat. Chem.*, 2014, **6**, 623–628.
12 T. G. Hsu, J. Zhou, H. W. Su, B. R. Schrage, C. J. Ziegler and J. Wang, *J. Am. Chem. Soc.*, 2020, **142**, 2100–2104.
13 Y. Lin, T. B. Kouznetsova and S. L. Craig, *J. Am. Chem. Soc.*, 2020, **142**, 2105–2109.
14 X. Hu, T. Zeng, C. C. Husic and M. J. Robb, *ACS Cent. Sci.*, 2021, **7**, 1216–1224.
15 M. B. Larsen and A. J. Boydston, *J. Am. Chem. Soc.*, 2013, **135**, 8189–8192.
16 M. B. Larsen and A. J. Boydston, *Macromol. Chem. Phys.*, 2016, **217**, 354–364.
17 M. A. Ghanem, A. Basu, R. Behrou, N. Boechler, A. J. Boydston, S. L. Craig, Y. Lin, B. E. Lynde, A. Nelson, H. Shen and D. W. Storti, *Nat. Rev. Mater.*, 2021, **6**, 84–98.
18 Z. Shi, J. Wu, Q. Song, R. Göstl and A. Herrmann, *J. Am. Chem. Soc.*, 2020, **142**, 14725–14732.
19 Y. Zhang, J. Yu, H. N. Bomba, Y. Zhu and Z. Gu, *Chem. Rev.*, 2016, **116**, 12536–12563.
20 K. S. Suslick, *Science*, 1990, **247**, 1439–1445.
21 G. Cravotto, E. C. Gaudinoa and P. Cintas, *Chem. Soc. Rev.*, 2013, **42**, 7521–7534.
22 K. Kooiman, H. J. Vos, M. Versluis and N. De Jong, *Adv. Drug Delivery Rev.*, 2014, **72**, 28–48.
23 S. Ibsen, A. Tong, C. Schutt, S. Esener and S. H. Chalasani, *Nat. Commun.*, 2015, **6**(6), 8264.
24 Y. Pan, S. Yoon, J. Sun, Z. Huang, C. Lee, M. Allen, Y. Wu, Y. J. Chang, M. Sadelain, K. Kirk Shung, S. Chien and Y. Wang, *Proc. Natl. Acad. Sci. U. S. A.*, 2018, **115**, 992–997.
25 P. N. T. Wells, *Phys. Med. Biol.*, 2006, **51**, R83.

© 2022 The Author(s). Published by the Royal Society of Chemistry

Open Access Article. Published on 16 March 2022. Downloaded on 2/9/2026 10:15:19 PM. This article is licensed under a Creative Commons Attribution-NonCommercial 3.0 Unported Licence.

26 J. Gonzales, R. K. Nair, S. J. Madsen, T. Krasieva and H. Hirschberg, *J. Biomed. Opt.*, 2016, **21**, 078002.
27 I. Lentacker, S. C. De Smedt and N. N. Sanders, *Soft Matter*, 2009, **5**, 2161–2170.
28 S. Dabral, H. Wotruba, J. G. Hernández and C. Bolm, *ACS Sustainable Chem. Eng.*, 2018, **6**, 3242–3254.
29 A. Stolle, T. Szuppa, S. E. S. Leonhardt and B. Ondruschka, *Chem. Soc. Rev.*, 2011, **40**, 2317–2329.
30 J. Li, C. Nagamani and J. S. Moore, *Acc. Chem. Res.*, 2015, **48**, 2181–2190.
31 J. Ayarza, Z. Wang, J. Wang, C.-W. Huang and A. P. Esser-Kahn, *ACS Macro Lett.*, 2020, 1237–1248.
32 S. Tu, Y. Guo, Y. Zhang, C. Hu, T. Zhang, T. Ma and H. Huang, *Adv. Funct. Mater.*, 2020, **30**, 1–31.
33 M. B. Starr and X. Wang, *Nano Energy*, 2015, **14**, 296–311.
34 M. Wang, B. Wang, F. Huang and Z. Lin, *Angew. Chem., Int. Ed.*, 2019, **58**, 7526–7536.
35 A. Cafarelli, A. Marino, L. Vannozzi, J. Puigmartí-Luis, S. Pané, G. Ciofani and L. Ricotti, *ACS Nano*, 2021, **15**, 11066–11086.
36 P. Christen, K. Ito, R. Ellouz, S. Boutroy, E. Sornay-Rendu, R. D. Chapurlat and B. Van Rietbergen, *Nat. Commun.*, 2014, **5**, 4855.
37 R. J. Nims, L. Pferdehirt, N. B. Ho, A. Savadipour, J. Lorentz, S. Sohi, J. Kassab, A. K. Ross, C. J. O'conor, W. B. Liedtke, B. Zhang, A. L. Mcnulty and F. Guilak, *Sci. Adv.*, 2021, **7**, 9858–9885.
38 S. Li, Z. Zhao, J. Zhao, Z. Zhang, X. Li and J. Zhang, *ACS Appl. Nano Mater.*, 2020, **3**, 1063–1079.
39 M. B. Starr, J. Shi and X. Wang, *Angew. Chem., Int. Ed.*, 2012, **51**, 5962–5966.
40 Z. Liang, C. F. Yan, S. Rtimi and J. Bandara, *Appl. Catal., B*, 2019, **241**, 256–269.
41 J. M. Wu, Y.-G. Sun, W.-E. Chang and J.-T. Lee, *Nano Energy*, 2018, **46**, 372–382.
42 R. Caliò, U. Rongala, D. Camboni, M. Milazzo, C. Stefanini, G. de Petris and C. Oddo, *Sensors*, 2014, **14**, 4755–4790.
43 H. Mohapatra, M. Kleiman and A. P. Esser-Kahn, *Nat. Chem.*, 2017, **9**, 135–139.
44 Z. Wang, J. Ayarza and A. P. Esser-Kahn, *Angew. Chem., Int. Ed.*, 2019, **58**, 12023–12026.
45 Z. Wang, X. Pan, L. Li, M. Fantin, J. Yan, Z. Wang, Z. Wang, H. Xia and K. Matyjaszewski, *Macromolecules*, 2017, **50**, 7940–7948.
46 Z. Wang, X. Pan, J. Yan, S. Dadashi-Silab, G. Xie, J. Zhang, Z. Wang, H. Xia and K. Matyjaszewski, *ACS Macro Lett.*, 2017, 546–549.
47 K. Kubota, Y. Pang, A. Miura and H. Ito, *Science*, 2019, **366**, 1500–1504.
48 Y. Pang, J. W. Lee, K. Kubota and H. Ito, *Angew. Chem., Int. Ed.*, 2020, **59**, 22570–22576.
49 C. Schumacher, J. G. Hernández and C. Bolm, *Angew. Chem., Int. Ed.*, 2020, **59**, 16357–16360.
50 N. Kvasovs and V. Gevorgyan, *Chem. Soc. Rev.*, 2021, **50**, 2244–2259.
51 I. Ghosh, L. Marzo, A. Das, R. Shaikh and B. König, *Acc. Chem. Res.*, 2016, **49**, 1566–1577.
52 P. P. Romańczyk and S. S. Kurek, *Electrochim. Acta*, 2020, 136404.
53 M. M. Chehimi, A. Lamouri, M. Picot and J. Pinson, *J. Mater. Chem. C*, 2014, **2**, 356–363.
54 R. Steeno, M. C. Rodríguez González, S. Eyley, W. Thielemans, K. S. Mali and S. De Feyter, *Chem. Mater.*, 2020, **32**, 5246–5255.
55 K. Matyjaszewski and J. Xia, *Chem. Rev.*, 2001, **101**, 2921–2990.
56 J. Chiefari, Y. K. Chong, F. Ercole, J. Krstina, J. Jeffery, T. P. T. Le, R. T. A. Mayadunne, G. F. Meijs, C. L. Moad, G. Moad, E. Rizzardo and S. H. Thang, *Macromolecules*, 1998, **31**, 5559–5562.
57 G. Moad, E. Rizzardo and S. H. Thang, *Aust. J. Chem.*, 2009, **62**, 1402–1472.
58 H. Zhou and J. A. Johnson, *Angew. Chem., Int. Ed.*, 2013, **52**, 2235–2238.
59 M. Chen, M. Zhong and J. A. Johnson, *Chem. Rev.*, 2016, **116**, 10167–10211.
60 T. G. McKenzie, Q. Fu, M. Uchiyama, K. Satoh, J. Xu, C. Boyer, M. Kamigaito and G. G. Qiao, *Adv. Sci.*, 2016, 1–9.
61 J. Xu, K. Jung, A. Atme, S. Shanmugam and C. Boyer, *J. Am. Chem. Soc.*, 2014, **136**, 5508–5519.
62 E. A. Merritt and B. Olofsson, *Angew. Chem., Int. Ed.*, 2009, **48**, 9052–9070.
63 B. M. Teo, M. Ashokkumar and F. Grieser, *J. Phys. Chem. B*, 2008, **112**, 5265–5267.
64 B. M. Teo, F. Grieser and M. Ashokkumar, *Macromolecules*, 2009, **42**, 4479–4483.
65 T. G. McKenzie, F. Karimi, M. Ashokkumar and G. G. Qiao, *Chem.–Eur. J.*, 2019, 1–18.
66 J. Collins, T. G. McKenzie, M. D. Nothling, S. Allison-Logan, M. Ashokkumar and G. G. Qiao, *Macromolecules*, 2018, **52**, 185–195.
67 J. Collins, T. G. McKenzie, M. D. Nothling, M. Ashokkumar and G. G. Qiao, *Polym. Chem.*, 2018, **9**, 2562–2568.
68 T. G. McKenzie, E. Colombo, Q. Fu, M. Ashokkumar and G. G. Qiao, *Angew. Chem., Int. Ed.*, 2017, **56**, 12302–12306.
69 Z. Wang, Z. Wang, X. Pan, L. Fu, S. Lathwal, M. Olszewski, J. Yan, A. E. Enciso, Z. Wang, H. Xia and K. Matyjaszewski, *ACS Macro Lett.*, 2018, 275–280.
70 J. Collins, T. G. McKenzie, M. D. Nothling, S. Allison-Logan, M. Ashokkumar and G. G. Qiao, *Macromolecules*, 2019, **52**, 185–195.
71 J. B. Ravnsbæk and T. M. Swager, *ACS Macro Lett.*, 2014, **3**, 305–309.
72 G. S. Lee, B. R. Moon, H. Jeong, J. Shin and J. G. Kim, *Polym. Chem.*, 2019, **10**, 539–545.
73 S. Grätz and L. Borchardt, *RSC Adv.*, 2016, **6**, 64799–64802.
74 N. Ohn, J. Shin, S. S. Kim and J. G. Kim, *ChemSusChem*, 2017, **10**, 3529–3533.
75 O. Maurin, P. Verdié, G. Subra, F. Lamaty, J. Martinez and T. X. Métro, *Beilstein J. Org. Chem.*, 2017, **13**, 2087–2093.
76 M. Hasegawa, Y. Akiho and Y. Kanda, *J. Appl. Polym. Sci.*, 1995, **55**, 297–304.
77 H. Y. Cho and C. W. Bielawski, *Angew. Chem., Int. Ed.*, 2020, **59**, 13929–13935.

Open Access Article. Published on 16 March 2022. Downloaded on 2/9/2026 10:15:19 PM.
This article is licensed under a Creative Commons Attribution-NonCommercial 3.0 Unported Licence.

78 G. A. Bowmaker, *Chem. Commun.*, 2013, **49**, 334–348.
79 H. Mohapatra, J. Ayarza, E. Sanders, A. M. Scheuermann, P. Griffin and A. P. Esser-Kahn, *Angew. Chem., Int. Ed.*, 2018, 11208–11212.
80 Z. Wang, J. Wang, J. Ayarza, T. Steeves, Z. Hu, S. Manna and A. P. Esser-Kahn, *Nat. Mater.*, 2021, **20**, 869–874.
81 J. Ayarza, Z. Wang, J. Wang and A. P. Esser-Kahn, *ACS Macro Lett.*, 2021, **10**, 799–804.
82 A. Bagheri and J. Jin, *ACS Appl. Polym. Mater.*, 2019, **1**, 593–611.
83 M. H. Shaw, J. Twilton and D. W. C. MacMillan, *J. Org. Chem.*, 2016, **81**, 6898–6926.

© 2022 The Author(s). Published by the Royal Society of Chemistry